CHEN, L., WANG, S., CHEN, L., QIAO, J. and FERNANDEZ, C. 2024. High-precision state of charge estimation of lithium-ion batteries based on improved particle swarm optimization-backpropagation neural network-dual extended Kalman filtering. *International journal of circuit theory and application* [online], 52(3), pages 1192-1209. Available from: https://doi.org/10.1002/cta.3788

High-precision state of charge estimation of lithium-ion batteries based on improved particle swarm optimization-backpropagation neural network-dual extended Kalman filtering.

CHEN, L., WANG, S., CHEN, L., QIAO, J. and FERNANDEZ, C.

2024

International Journal of
Circuit Theory and Applications

High-precision SOC estimation of Lithium-ion batteries based on improved particle swarm optimization-back propagation neural network-dual extended Kalman filtering

Journal:	*International Journal of Circuit Theory and Applications*
Manuscript ID	CTA-23-0310.R1
Wiley - Manuscript type:	Original Article
Date Submitted by the Author:	19-Jul-2023
Complete List of Authors:	Chen, Lu; Southwest University of Science and Technology; Sichuan University College of Electrical Engineering Wang, Shunli; Southwest University of Science and Technology; Sichuan University College of Electrical Engineering Chen, Lei; Southwest University of Science and Technology Qiao, Jialu; Southwest University of Science and Technology; Sichuan University College of Electrical Engineering Fernandez, Carlos; Robert Gordon University School of Pharmacy and Life Sciences
Keyword:	<i>Double extended Kalman filter</i>, <i>Backpropagation neural network</i>, <i>Particle swarm optimization algorithm</i>, <i>Estimation of state of charge</i>, <i>Ternary lithium battery</i>

High-precision SOC estimation of Lithium-ion batteries based on improved particle swarm optimization-back propagation neural network-dual extended Kalman filtering

Lu Chen[a,b], Shunli Wang[a*,b], Lei Chen[a], Jialu Qiao[a,b], Carlos Fernandez[c]

([a] School of Information Engineering, Southwest University of Science and Technology, Mianyang 621010, China;[b] College of Electrical Engineering, Sichuan University, Chengdu 610065, China;[c] School of Pharmacy and Life Sciences, Robert Gordon University, Aberdeen AB10-7GJ, UK)

Abstract: High precision state of Charge (SOC) estimation is essential for battery management systems (BMS). In this paper, a new SOC estimation method is proposed. The dual Kalman filter algorithm is combined with the back-propagation neural network (PSO-BPNN-DEKF) which optimizes the initial weights and thresholds by particle swarm optimization algorithm to estimate and correct the SOC of lithium-ion batteries. Based on the second-order RC equivalent circuit model, parameter identification is carried out using the adaptive forgetting factor least squares method (AFFRLS). Implement online parameter updates and SOC estimation through the DEKF algorithm. Then, the trained PSO-BPNN is used to predict the SOC estimation error in real time, and the SOC estimation value is corrected by adding prediction errors. The SOC estimates before and after correction under Beijing Dynamic Stress Test (BBDST), dynamic Stress Test (DST), and Hybrid Pulse Power Characterization(HPPC) were compared. Under BBDST, DST, and HPPC tests, the maximum errors of the corrected SOC estimates are 0.0107, 0.0090, and 0.0147, respectively. The root mean square error (RMSE) of the corrected SOC estimates decreased by 94.02%, 83.18%, and 88.03% respectively compared with the EKF. The MAE of the corrected SOC estimates remained around 0.1% for all the BBDST dynamic operating conditions at different temperatures. The experimental results demonstrate the accuracy, effectiveness, and temperature adaptability of the proposed algorithm for SOC estimation under complex conditions of lithium-ion batteries.

Keywords: *Double extended Kalman filter; Backpropagation neural network; Particle swarm optimization algorithm; Estimation of state of charge; Ternary lithium battery*

Corresponding author: *Shunli Wang. Tel/fax: +86-15884655563. E-mail address: wangshunli@swust.edu.cn.*

1. Introduction

As a clean and reusable energy source, the lithium-ion battery has advantages such as high power and energy density, long life, good design flexibility, and no memory effect, and has become the most promising energy storage device for electric vehicles[1]. In real-time EV applications, a battery management system (BMS) is needed to monitor the internal state of the battery to ensure the best use of lithium-ion batteries[2]. As one of the key technologies for EV battery management, the estimation of the battery state of charge plays an important role in battery protection and service life prediction[3]. However, due to its nonlinear characteristics, accurate estimation of battery SOC is a key challenge for BMS[4].

With the increasing requirement for SOC estimation accuracy, the research on real-time SOC estimation methods for lithium batteries is developing toward the trend of model diversification and algorithm complexity[5]. At present, common SOC estimation methods include amp-hour integration method[6, 7], open-circuit voltage method[8, 9], Kalman filter algorithm[10-12], support vector machine[13-15] and neural network algorithm[16, 17], etc. Among them, the Ah integral algorithm is the most commonly used method[18]. However, due to the problems of initial SOC measurement and accumulation error, it is usually combined with other methods[19]. Zhang Xin, Hou Keywei, et al proposed the GWO-BP optimized amp-hour integral method to keep the estimation error of the SOH-SOC joint estimation model within 5% [18]. The author proposed a fusion algorithm of F-EKF-Ah and utilized the advantage of the EKF algorithm's high estimation accuracy in the nonlinear interval to solve the error problem caused by the inaccurate initial value of the Ah integral algorithm[20]. Meanwhile, the development of deep learning provides an emerging solution for SOC estimation[21]. As a data-driven method to solve the SOC estimation problem of lithium batteries, deep learning has the advantages of high precision and short modeling time[22]. The author proposes a stacked bidirectional long and short-term memory (SBLSTM) neural network for SOC estimation, which makes full use of battery time information to estimate SOC value [23]. Fan, XY proposed the boundary effect of symmetric convolutional neural networks (CNN) to improve the accuracy of edge SOC estimation[24]. However, the success of neural networks in SOC estimation depends on the assumption that training data and test data have the same distribution, which is heavily dependent on data[25]. The model-based filtering method is widely used in practical engineering due to its advantages of high precision, closed-loop, strong self-correction ability, and adaptive ability[26]. Li Lulu established a second-order fractional electrical model of lithium battery based on the second-order RC equivalent circuit model and then adopted a traceless particle algorithm based on Schmidt orthogonal transformation idea for state estimation, which improved the robustness and computational efficiency of the algorithm[27]. Zhang Xiaoyang proposed an adaptive extended Kalman particle filter based on the hierarchical model for SOC estimation, which further improved the accuracy and robustness of SOC estimation based on reducing the computational burden[28]. A general battery model based on differential voltage (DV) analysis and two SOC estimation algorithms based on EKF and particle filter (PF) is proposed to achieve SOC estimates with a maximum absolute error of 1.75% and root mean square error of less than 1.10% [29]. Reference[30] proposed an improved adaptive Kalman filter algorithm to achieve co-estimation of battery capacitance and SOC. Considering the effect of temperature on OCV, the online OCV identified by FFRLS is innovatively taken as the observation state to improve the SOC estimation accuracy, but the effect of battery aging is ignored in this method. Reference[31] proposed an improved adaptive fifth-order cubature Kalman filter for real-time SOC estimation. Adopted fading filter and square root filter to improve the robustness, which greatly improved the SOC estimation accuracy. But the accuracy of such methods depends on the accuracy of the battery model. Therefore, it is also very important to improve the accuracy of the battery model and parameter identification[32]. The equivalent circuit model of the battery model is the most widely used to characterize battery characteristics through a specific circuit[33]. At present, battery-equivalent circuit models mainly include the Rint model, PNGV model, Thevenin model, and nth-order RC equivalent circuit model[34]. Among them, the nth-order RC equivalent model has higher precision, and usually the more RC links, the higher the accuracy, but the more complex the calculation, so it is not suitable for the system with high real-time performance and limited hardware conditions[35]. The second-order RC equivalent circuit model is widely used because of its good accuracy and dynamic simulation characteristics, low circuit model complexity, and low computational burden[36]. At the same time, in order to improve the accuracy of battery model parameters, online parameter identification is usually adopted to obtain battery model parameters, among which recursive least squares algorithm and its derivative algorithm are the most widely used[37]. Some studies also improve SOC estimation accuracy by improving model accuracy.In reference[38], SOC estimation was performed based on FOM, which improved the accuracy of SOC estimation. Reference[39] uses a second-order RC equivalent circuit with a thermal model for simulation, taking into account the influence of temperature on SOC estimation accuracy, and improving the temperature adaptability of SOC estimation.

With the vigorous development of the new energy automobile industry, the requirement for SOC estimation accuracy is constantly increasing. A new design idea for the SOC estimation method is proposed. Reference[40] combines machine learning with Kalman filtering algorithms. The characteristic variables obtained by the Kalman filter algorithm are used as input variables for SOC estimation, which provides a new idea for the design of a battery condition monitoring scheme. In this study, combining the advantages of model-based methods and deep learning algorithms, a particle swarm optimization back propagation neural network correction Double Kalman filter (PSO-BPNN-DEKF) method is proposed for high-precision SOC estimation. The main contributions of this study include. (1) We are modeling the battery based on the second-order RC equivalent circuit model. A simple adaptive forgetting factor least square method is proposed to identify model parameters, which improves the accuracy of model parameter identification. (2) we proposed a new method of high-accuracy of SOC estimation. Firstly, the cyclic update of the DEKF algorithm is used for SOC estimation and real-time update of model parameters, which reduces the impact of time-varying parameters on SOC estimation accuracy in complex working environments. Then, the trained PSO-BPNN is introduced to predict the SOC estimation error in real-time. The SOC estimation results of DEKF are corrected by adding the error, to further improve the SOC estimation accuracy. (3) We put forward a detailed derivation process of DEKF theory, which is easy for researchers to understand and apply. (4) The effectiveness and accuracy of the proposed method are verified under BBDST, DST, and HPPC working conditions. It lays a theoretical foundation for the condition monitoring of lithium batteries.

The content of this paper is organized as follows. In the second section of mathematical analysis, the battery model and parameter identification, SOC estimation of DEKF, and SOC correction of PSO-BPNN are introduced. In the third section, the experimental results under three complex conditions and different temperatures are analyzed. The fourth section summarizes the thesis.

2. *Mathematical analysis*

2. 1. Equivalent circuit modeling

The SOC estimation based on the Kalman filter algorithm needs to be based on an accurate battery model. The second-order RC equivalent circuit model is widely used in various equivalent circuits because of its high precision. Therefore, the second-order RC circuit was used in this study to model the battery, and the equivalent model is shown in Figure 1.

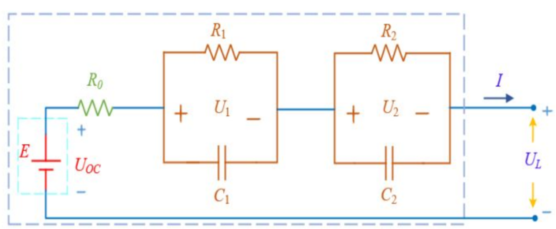

Figure 1. Second Order RC Equivalent Circuit model.

According to Kirchhoff's Law, the model equation can be obtained as Equation (1).

$$\begin{cases} U_{oc} = U_0 + \mathrm{IR}_0 + U_1 + U_2 \\ \dfrac{dU_1}{d_t} = -\dfrac{U_1}{R_1C_1} + \dfrac{I}{C_1} \\ \dfrac{dU_2}{d_t} = -\dfrac{U_2}{R_2C_2} + \dfrac{I}{C_2} \end{cases} \quad (1)$$

The SOC expression of the battery is shown in Equation (2).

$$\mathrm{SOC}(t) = SOC_0 - \frac{\gamma I \Delta t}{C_n} \quad (2)$$

Among them, R_0 is ohm internal resistance, R_1 and C_1 are electrochemical polarization resistance and capacitance respectively, R_2 and C_2 are concentration polarization resistance and capacitance respectively, U_{oc} is open circuit voltage, U_L is terminal voltage, and I is battery operating current. γ is the Coulomb efficiency, $\gamma = 1$, SOC_0 is the initial value, Δt is the sampling time, C_n is the actual capacity of the battery.

According to Equation (1), the equation of state is obtained by discretization, as shown in Equation (3).

$$\begin{cases} \begin{bmatrix} SOC(k+1) \\ U_1(k+1) \\ U_2(k+1) \end{bmatrix} = \begin{bmatrix} 1 & 0 & 0 \\ 0 & e^{-\frac{1}{R_1C_1}} & 0 \\ 0 & 0 & e^{-\frac{1}{R_2C_2}} \end{bmatrix} \begin{bmatrix} SOC(k) \\ U_1(k) \\ U_2(k) \end{bmatrix} + \begin{bmatrix} -\frac{\Delta t}{C_n} \\ \mathrm{R}_1\left(1-e^{-\frac{1}{R_1C_1}}\right) \\ \mathrm{R}_2\left(1-e^{-\frac{1}{R_2C_2}}\right) \end{bmatrix} i_k \\ U_L(k+1) = U_{\mathrm{oc}}(\mathrm{SOC},\ k+1) - U_1(k+1) - U_2(k+1) - \mathrm{R}_0 i_{k+1} \end{cases} \# \quad (3)$$

Among them, the expression of the time constant is $\tau_1 = \mathrm{R}_1 C_1$, $\tau_2 = \mathrm{R}_2 C_2$. The relationship between open circuit voltage U_{oc} and SOC can be obtained by fitting.

Open circuit voltage(OCV) refers to the potential difference between the poles of a battery when it is not discharging. Determining the OCV-SOC relationship is an indispensable step in SOC estimation based on the battery model. The mathematical relationship of OCV-SOC is realized by the HPPC test. In the HPPC test, the open-circuit voltage values corresponding to each interval of 0.1 in the SOC from 0 to 1 are recorded. The 11 sets of recorded data were then used to fit the OCV polynomial concerning SOC. The target polynomial is shown in Equation (4).

$$\mathrm{OCV}(SOC) = c_0 + \sum_{n=1}^{n} c_n \times SOC^n \# (4)$$

2.2. AFFRLS Parameter identification

The least square method (LS) is one of the most commonly used estimation methods in system identification. To overcome the problem of "data saturation" in this method, the forgetting factor is introduced. Thus, the influence of old data on new data prediction is weakened to improve the identification accuracy. However, when the charging and discharging current changes frequently, the fixed forgetting factor will affect the dynamic recognition ability and accuracy of circuit parameters. Therefore, a simple adaptive forgetting factor formula is proposed in this paper, which can make the forgetting factor self-adjust within a certain range, to improve the dynamic recognition ability and accuracy of circuit parameters.

According to Equation (1), the Laplace equation of the battery model is shown in Equation (5).

$$E = U_{\mathrm{oc}}(\mathrm{s}) - U_L(\mathrm{s}) = \left(\frac{R_1}{R_1C_1s+1} + \frac{R_2}{R_2C_2s+1} + \mathrm{R}_0\right) I(s) \# \quad (5)$$

Rewrite expression (5) as expression (6).

$$G(s)=\frac{E(s)}{I(s)}=\left(\frac{R_1}{R_1C_1s+1}+\frac{R_2}{R_2C_2s+1}+R_0\right)\# \quad (6)$$

Substitute the time constant $\tau_1=\mathrm{R}_1C_1$, $\tau_2=\mathrm{R}_2C_2$ into Equation (6). Discretization by bilinear transformation, set $s=\frac{2}{T}\times\frac{1-\mathrm{Z}^{-1}}{1+\mathrm{Z}^{-1}}$ get the form of transfer function such as formula (7).

$$G(\mathrm{Z}^{-1})=\frac{E(k)}{I(k)}=\frac{k_3+k_4\mathrm{Z}^{-1}+k_5\mathrm{Z}^{-2}}{1-k_1\mathrm{Z}^{-1}-k_2\mathrm{Z}^{-2}}\#(7)$$

Among them, k_1, k_2, k_3, k_4, k_5 are the corresponding constant coefficients. *I(k)* and *E(k)* are the input and output of the system respectively. Convert equation (7) into a differential equation such as equation (8).

$$E(k)=k_1E(k-1)+k_2E(k-2)+k_3I(k)+k_4I(k-1)+k_5(k-2)\#(8)$$

Set $a=\tau_1\tau_2$, $b=\tau_1+\tau_2$, $\mathrm{c}=\mathrm{R}_1+\mathrm{R}_2+\mathrm{R}_0$, $\mathrm{d}=\mathrm{R}_1\tau_2+\mathrm{R}_2\tau_1+\mathrm{R}_0(\tau_1+\tau_2)$

Among them,

$$\begin{cases} k_1=\dfrac{8a-2T^2}{T^2+2bT+4a} \\ k_2=\dfrac{4bT}{T^2+2bT+4a}-1 \\ k_3=-\dfrac{cT^2+2dT+4a\mathrm{R}_0}{T^2+2bT+4a} \\ k_4=\dfrac{8a\mathrm{R}_0-2cT^2}{T^2+2bT+4a} \\ k_5=-\dfrac{cT^2-2dT+4a\mathrm{R}_0}{T^2+2bT+4a} \end{cases}\# \quad (9)$$

As shown in equation (9) above, let $\theta=[k_1,k_2,k_3,k_4,k_5]^T$, θ is the coefficient to be identified. Set the sampling error of the sensor at moment *k* as *e(k)*, and equation (10) can be obtained.

$$\mathrm{E}(k)=\phi^T(k)\theta+\mathrm{e}(k)\#(10)$$

Parameters are identified through the least squares algorithm of the forgetting factor. The recursive process of the least squares algorithm of the forgetting factor is shown in Equation (11).

$$\begin{cases} \hat{\theta}(k)=\hat{\theta}(k-1)+K(k)\left[E(k)-\phi^T(k)\hat{\theta}(k-1)\right] \\ K(k)=P(k-1)\phi(k)\left[\phi^T(k)P(k-1)\phi(k)+\lambda\right]^{-1} \\ P(k)=\lambda^{-1}\left[I-K(k)\phi^T(k)P(k-1)\right] \end{cases}\# \quad (11)$$

Among them, $P(k)$ is the covariance matrix, $\phi(k)=[E(k),E(k-1),I(k),I(k-1),I(k-2)]$, K is the gain, λ is the forgetting factor, on behalf of the distribution of the weight of the old and new data. λ ranges from $0<\lambda<1$ usually taking the constant of 0.98. The smaller the value of λ, the better the tracking performance of the algorithm, but it also increases the possibility of oscillation.

When the error of parameter identification is very small, the forgetting factor should be close to 1. When the online parameter identification error is large, the forgetting factor should be reduced to accelerate the convergence speed and reduce the identification error. Therefore, we expect that the forgetting factor can be adjusted adaptively with the error of parameter identification. Therefore, a simple Equation (12) for calculating the adaptive forgetting factor is proposed as follows.

$$\begin{cases} \lambda(k) = \lambda_{min} + (1 - \lambda_{min})\mu^{\alpha(k)} \\ \alpha(k) = round\left(\frac{e(k)}{e_{set}}\right)^2 \end{cases} \# \quad (12)$$

Among them, λ_{min} is the minimum value of the forgetting factor, $\mu$is the sensitivity coefficient, indicating the sensitivity of the forgetting factor to error. $e(k)$ is the error at time k, $e_{set}$is the allowable error reference.

By iterative calculation, θ can be obtained for each calculation. Then the values of R_0, R_1, R_2, C_1, C_2 can be calculated.

2.3 PSO-BPNN-DEKF algorithm

Battery model parameters are unstable and change with complex working conditions. To reduce the SOC estimation error caused by the instability of model parameters, it is necessary to identify model parameters online. DEKF algorithm was introduced to estimate battery SOC and model parameters by an iterative method. Real-time tracking and correction of model parameters can solve the problem of time-varying model parameters, which can effectively improve the accuracy of the battery model and SOC estimation accuracy. To further improve the accuracy of SOC estimation, trained PSO-BPNN is introduced to predict the SOC estimation error of the DEKF. Correction is achieved by adding prediction errors The PSO algorithm optimizes the initial weight and threshold of BPNN, and improves the prediction accuracy of the trained PSO-BPNN model, to further improve the correction accuracy. The flow chart of the proposed PSO-BPNN-DEKF algorithm is shown in Figure 2.

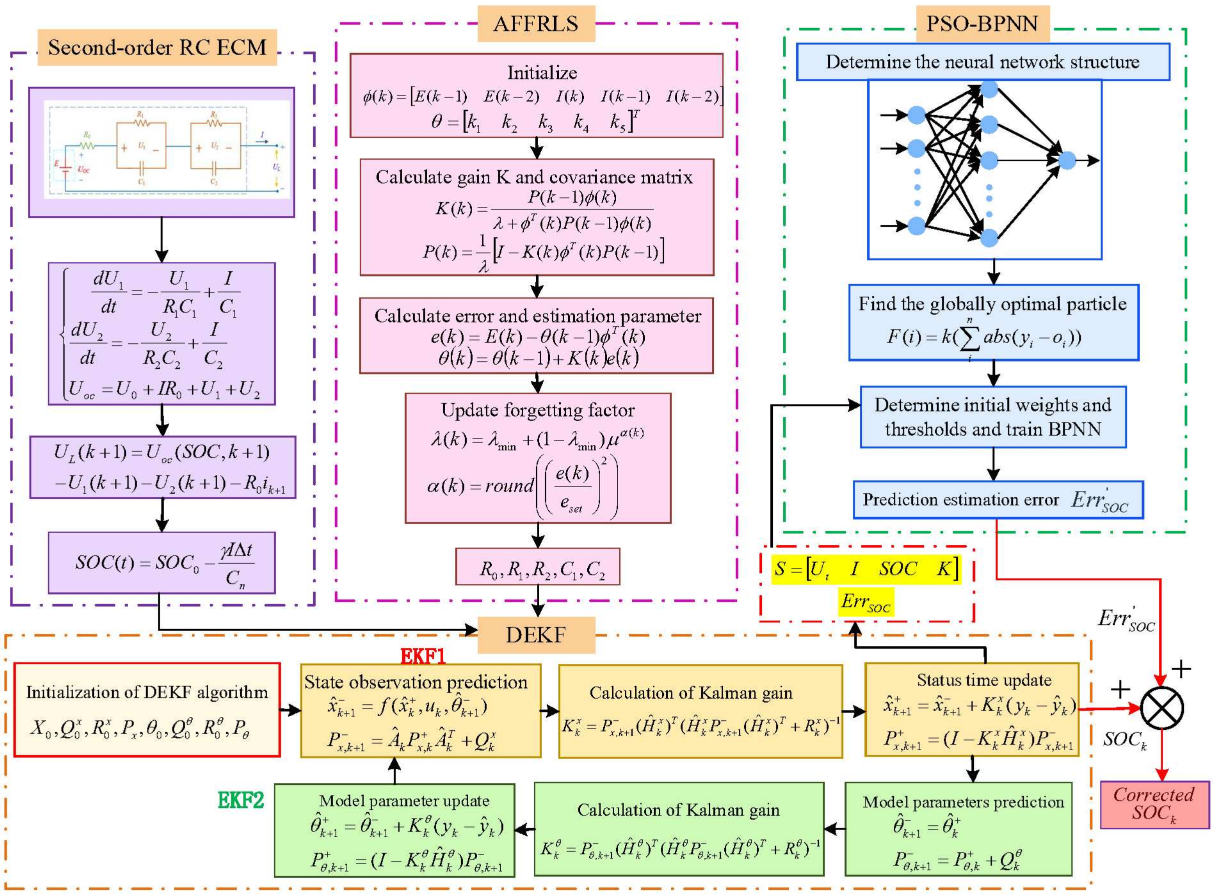

Figure 2. The flow chart of the PSO-BPNN-DEKF algorithm

2.3.1 DEKF algorithm principle

DEKF uses two EKFs respectively to estimate the SOC and internal parameters of the battery. SOC is used as input when estimating internal parameters. Similarly, when estimating SOC, the internal parameters are taken as inputs to establish mutually input state filters. The state-space equation of this model is shown in Equation (13).

$$\begin{cases} x_{k+1} = f(x_k,u_k,\theta_k) + w_k^x \\ y_k = g(x_k,u_k,\theta_k) + v_k^x \end{cases} \# \quad (13)$$

Among them, $x_k = [SOC(k),U_1(k),U_2(k)]^T$, Output is $y_k = U_L(k)$. The control variable is $u_k = I_k$. The process noise is $w_k^x \sim N(0,Q^x)$. The observed noise is $v_k^x \sim N(0,R^x)$.

θ_k is the system parameter vector, and the state-space expression of the model is shown in Equation (14).

$$\begin{cases} \theta_{k+1} = \theta_k + w_k^\theta \\ y_k = g(x_k,u_k,\theta_k) + v_k^\theta \end{cases} \# \quad (14)$$

Among them, $\theta_k = [R_0,R_1,C_1,R_2,C_2]^T$. The process noise is $w_k^\theta \sim N(0,Q^\theta)$. The observed noise is $v_k^\theta \sim N(0,R^\theta)$.

The steps of the DEKF algorithm are as follows.

Step 1: Initialize X_0, Q_0^x, R_0^x, P_x; θ_0, Q_0^θ, R_0^θ, P_θ.

Step 2: State observation prediction.

$$\hat{x}_{k+1}^{+} = f\left(\hat{x}_{k}^{+}, u_k, \hat{\theta}_{k+1}^{-}\right)\#(15)$$

$$P_{x,k+1}^{-} = \hat{A}_k P_{x,k}^{+} \hat{A}_k^{T} + Q_k^{x}\# \quad (16)$$

Step 3: Status time update.

$$K_k^x = P_{x,k+1}^{-}\left(\hat{H}_k^x\right)^T\left(\hat{H}_k^x P_{x,k+1}^{-}\left(\hat{H}_k^x\right)^T + R_k^x\right)^{-1}\# \quad (17)$$

$$\hat{x}_{k+1}^{+} = \hat{x}_{k+1}^{-} + K_k^x(y_k - \hat{y}_k)\# \quad (18)$$

$$P_{x,k+1}^{+} = \left(I - K_k^x \hat{H}_k^x\right) P_{x,k+1}^{-}\# \quad (19)$$

Step 4: Model parameters observation prediction.

$$\hat{\theta}_{\mathrm{k}+1}^{-} = \hat{\theta}_k^{+}\# \quad (20)$$

$$P_{\theta,k+1}^{-} = P_{\theta,k}^{+} + Q_k^{\theta}\# \quad (21)$$

Step 5: Model parameter update

$$K_k^{\theta} = P_{\theta,k+1}^{-}\left(\hat{H}_k^{\theta}\right)^T\left(\hat{H}_k^{\theta} P_{\theta,k+1}^{-}\left(\hat{H}_k^{\theta}\right)^T + R_k^{\theta}\right)^{-1}\# \quad (22)$$

$$\hat{\theta}_{k+1}^{+} = \hat{\theta}_{k+1}^{-} + K_k^{\theta}(y_k - \hat{y}_k)\# \quad (23)$$

$$P_{\theta,k+1}^{+} = \left(I - K_k^{\theta} \hat{H}_k^{\theta}\right) P_{\theta,k+1}^{-}\# \quad (24)$$

Where A_k, H_k^x and H_k^{θ} are the Jacobian matrix, and the expression is shown in (25).

$$\mathrm{A}_k \triangleq \frac{\partial f(x_k, u_k, \theta_k)}{\partial x}, H_k^x \triangleq \frac{\partial g(x_k, u_k, \theta_k)}{\partial x}, H_k^{\theta} \triangleq \frac{\partial \partial g(x_k, u_k, \theta_k)}{\partial \theta}\#(25)$$

The real-time model parameters and state variable SOC can be estimated by constantly updating the time state and observation state through equations (15)~(24).

2.3.2 PSO-BPNN correction

No matter what method is used to estimate SOC, there will be estimation errors. If the estimation error is known and the estimation error is added to the estimated value, the error correction can be realized, to get a more accurate estimator. However, because the input/output variables of the estimation error and estimator are highly nonlinear, the mathematical relationship between them cannot be described by a function. To solve this nonlinear problem, a neural network model is proposed to predict the estimation error. Among them, BPNN is widely used because of its strong nonlinear mapping ability and flexible network structure. However, BPNN also has some disadvantages. BPNN is easy to fall into the local minimum value, thus reducing the accuracy of the model prediction. Therefore, the PSO-BPNN model is proposed for error correction. The global optimization ability of the PSO algorithm is used to improve the generalization ability and learning performance of BPNN, and further improve the prediction accuracy of the PSO-BPNN model. The flow chart of the PSO-BPNN algorithm is shown in Figure 3, and the detailed process is as follows.

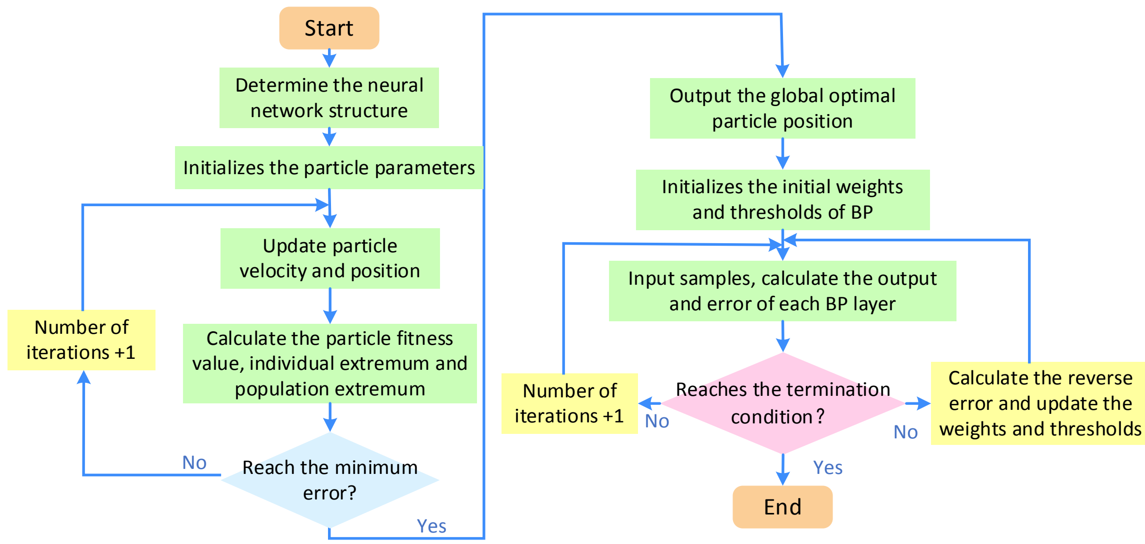

Figure 3. The flow chart of the PSO-BPNN algorithm

Step 1: First determine the structure hierarchy relationship of the BPNN algorithm, as well as the number of the input layer, hidden layer, and output layer, to determine the optimal parameters in the particle swarm optimization algorithm, and determine the number of particle swarm dimension according to the structure.

Step 2: Determine the fitness function in the particle swarm model.

Step 3: Set the initial value of particles in the particle swarm.

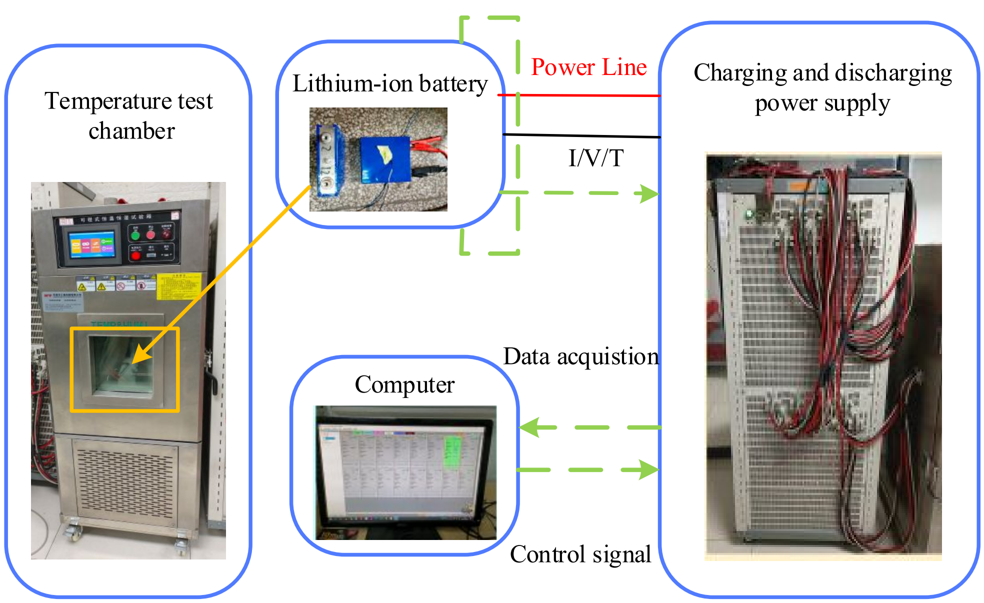

Figure. 4 Test platform structure drawing

Step 4: Find the optimal initial weight and threshold in BP neural network. In this paper, the fitness algorithm of the particle swarm is used to find the minimum value. Through this minimum value, the optimal position of the particle is found through continuous iterative calculation. The value corresponding to this position is the optimal initial value of the weight and threshold.

Step 5: Introduce the optimal initial weight and threshold determined in the previous step into the BP neural network model, and then start the prediction work.

3. *Experimental analysis*

3. 1 Experimental operating conditions

To verify the effectiveness of the PSO-BPNN-DEKF algorithm in SOC estimation, this study uses a terpolymer lithium battery with a rated capacity of 70Ah as the research object to carry out charging and discharging experiments. The experimental platform is shown in Figure 4. The whole experimental platform is composed of the host system, programmable thermostatic control box, ternary lithium-ion battery, and battery test system. The specific parameters of the lithium-ion battery used in the experiment are shown in Table 1.

Table 1. Lithium-ion battery specifications

Battery parameter	Value
Standard Capacity	70Ah
Maximum continuous discharge	3C
Nominal voltage	3.7V
Charging upper voltage	4.2V
Discharge lower limit voltage	2.75V
Size	149mm×98mm×1500mm

3.2. OCV-SOC relationship Curve

To obtain a more accurate OCV-SOC relationship, different order polynomials are used as the objective function for fitting. The RMSE of fitting polynomials of different orders as the objective function is shown in Table 2.

Table 2. RMSE distributions are fitted by polynomials of different orders

The highest order	1	2	3	4	5	6	7	8	9
RMSE (V)	0.0719	0.0761	0.0495	0.0212	0.0131	0.0143	0.0103	0.0036	0.0046

However, the higher the order of the target polynomial, the greater the amount of computation. After balancing the accuracy and computational effort of the fit, an 8th-order polynomial was chosen to fit the OCV(SOC) function.

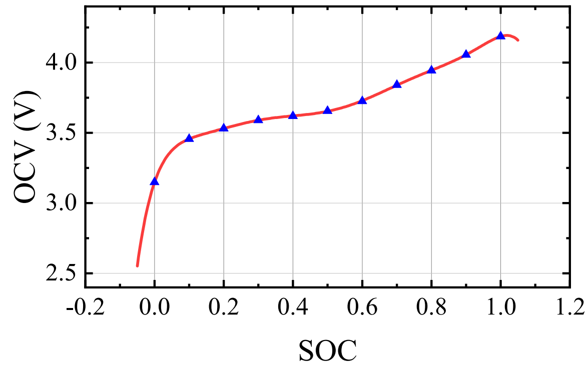

Figure 5. OCV-SOC fitting curve

The fitting curve of OCV-SOC is shown in Figure 5. It can be seen that SOC and the corresponding OCV points are very close to the fitting curve, and the fitting effect is relatively good, with RMSE only 0.0036V. The fitting polynomial coefficients are shown in Table 3.

Table 3. Values of polynomial fitting coefficients

Coefficient	Value
c_0	3.148
c_1	7.199
c_2	-70.61
c_3	404.8
c_4	-1326
c_5	2518
c_6	-2730
c_7	1567
c_8	-369.2

3. 3 Parameter identification result

The minimum adaptive change value of the forgetting factor is set to 0.98 so that the change range of the forgetting factor is 0.98~1. The measured current and voltage data in the BBDST condition were used for parameter identification. The whole discharge process time was 41533s, and the sampling interval time was 0.1s. AFFFRLS parameter identification results are shown in Figure 6. The average values of AFFRLS parameter identification are shown in Table 4. The results of AFFRLS parameter identification have obvious fluctuations, but also more accurately reflect the complex property of real-time changes of parameters with the change of charge and discharge current. There are also some spikes in the dynamic parameters, which fully highlight the recognition ability of frequent switching between charging and discharging current.

Tab. 4 AFFRLS parameter identification result

Parameter	R_0	R_1	R_2	C_1	C_2
Value	8.0230e-04Ω	0.0050Ω	1.226e-05Ω	1.4974+05F	6.6598+04F

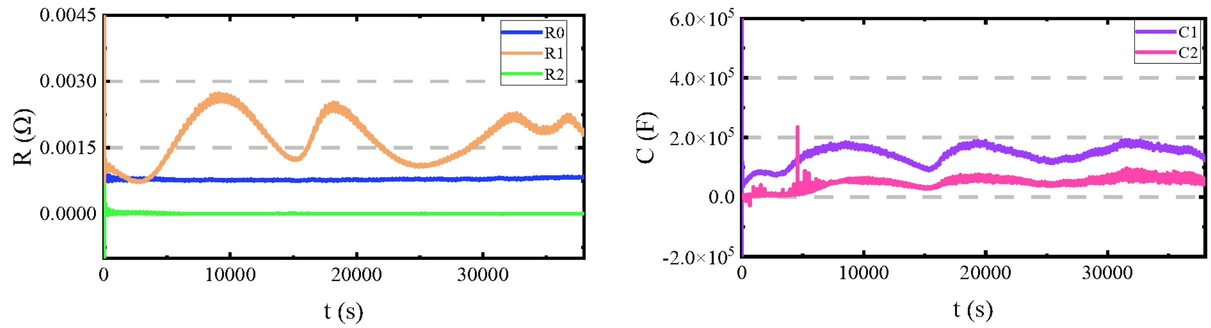

(a) Resistance identification curve (b) Capacity identification curve

Figure 6. Identification results of second-order RC circuit parameters based on AFFRLS

To verify the accuracy of the parameter identification results, the simulated output voltage of the model is compared with the measured voltage of the experiment. Terminal voltage estimation results and error curves are shown in Figure 7. The error of the predicted voltage is shown in Table 5.

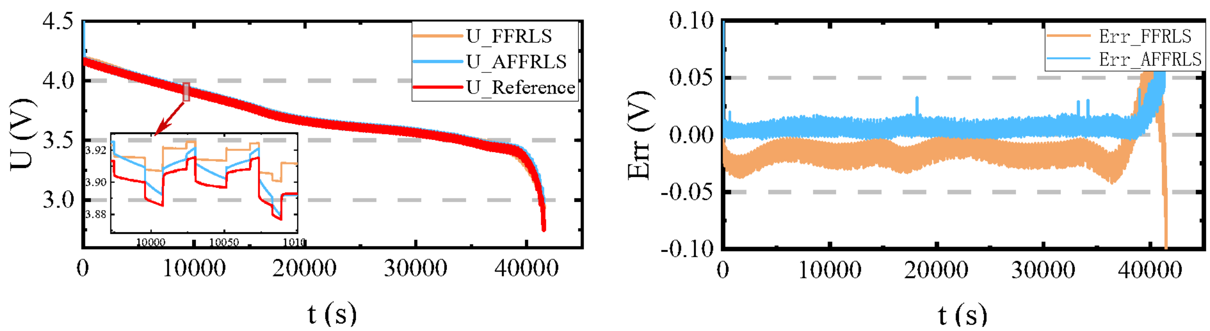

(a) voltage curve (b) AFFRLS simulation voltage error result curve

Figure 7. Second-order RC model voltage validation and error curve

Tab. 5 Voltage verification error of second order RC model under BBDST working condition

	MAE	RMSE	MAPE
FFRLS	0.0153V	0.0201V	0.0042
AFFRLS	0.0078V	0.0128V	0.0022

The output analog voltage of the model identified by AFFRLS is closer to the measured value. MAE and RMSE were 0.0078V and 0.0128V respectively under BBDST conditions. Large voltage errors occurred only at the end of the BBDST test phase. This phenomenon is caused by the unstable dynamic characteristics of the battery under the condition of a full discharge. BBDST verification experiment results show that the AFFRLS algorithm has higher accuracy and higher reliability in parameter identification.

3. 4 Training and testing of PSO-BPNN

In this paper, the proposed PSO-BPNN corrects SOC estimates. Before the correction, the PSO-BPNN model needs to be trained to get the best model. The training samples were obtained from SOC estimation results under DST and BBDST conditions and HPPC tests with DEKF. To obtain a more suitable BPNN model, BPNN with a single hidden layer with a different number of neurons is constructed, and then the same samples are used to train PSO-BPNN with a different number of neurons. The training MSE of PSO-BPNN with a different number of neurons is shown in Figure 8. It can be seen that the prediction effect is best when the number of hidden layer neurons is 13. Therefore, a single hidden layer PSO-BPNN with 13 neurons was selected for error prediction in this study. The PSO-BPNN was tested to verify its performance through the test samples under BBDST conditions. The predicted results of the test are shown in Figure 9.

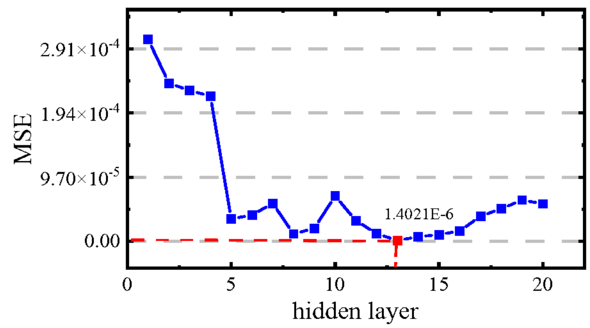

Figure 8. The training MSE of PSO-BPNN with different number of neurons

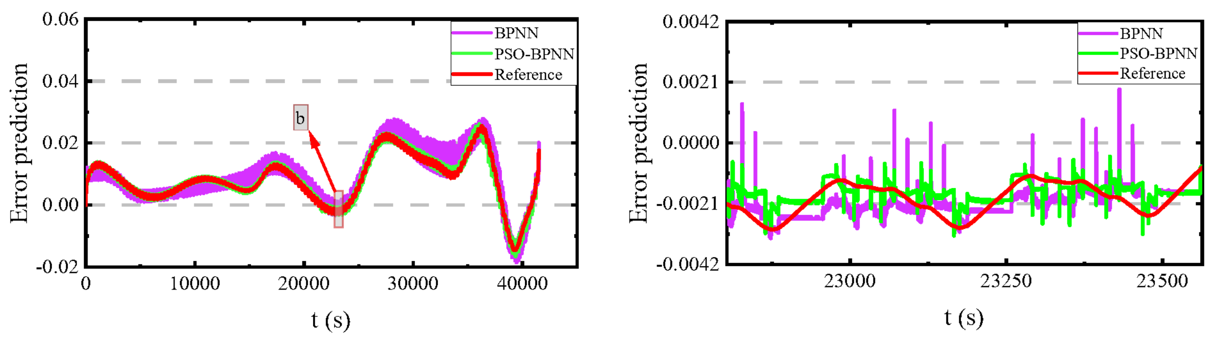

(a) SOC error prediction results (b) Local magnification of SOC error prediction results

Figure 9. Prediction effect curve of PSO-BPNN under BBDST condition

According to the test results, the validity and effectiveness of the PSO-BPNN model can be verified. The error predicted by PSO-BPNN is very close to the SOC estimation error and even has good consistency in the place where the error fluctuation is drastic. BPNN predicts MAE and RMSE of 0.11% and 0.14%, respectively. MAE and RMSE were 3.3509e-04 and 4.4703e-04, respectively, predicted by PSO-BPNN. It can be seen that the accuracy and superiority of PSO-BPNN error prediction.

3. 5 SOC estimation results based on PSO-BPNN-DEKF

3.5.1 SOC estimation results under different working conditions

The trained PSO-BPNN corrects the error of the SOC estimated by DEKF to obtain a more accurate SOC estimate. The effectiveness of the PSO-BPNN-DEKF algorithm is verified by the experimental data of BBDST, DST, and HPPC tests at 25℃. The estimation curve and error curve under BBDST working condition is shown in Figure

10.

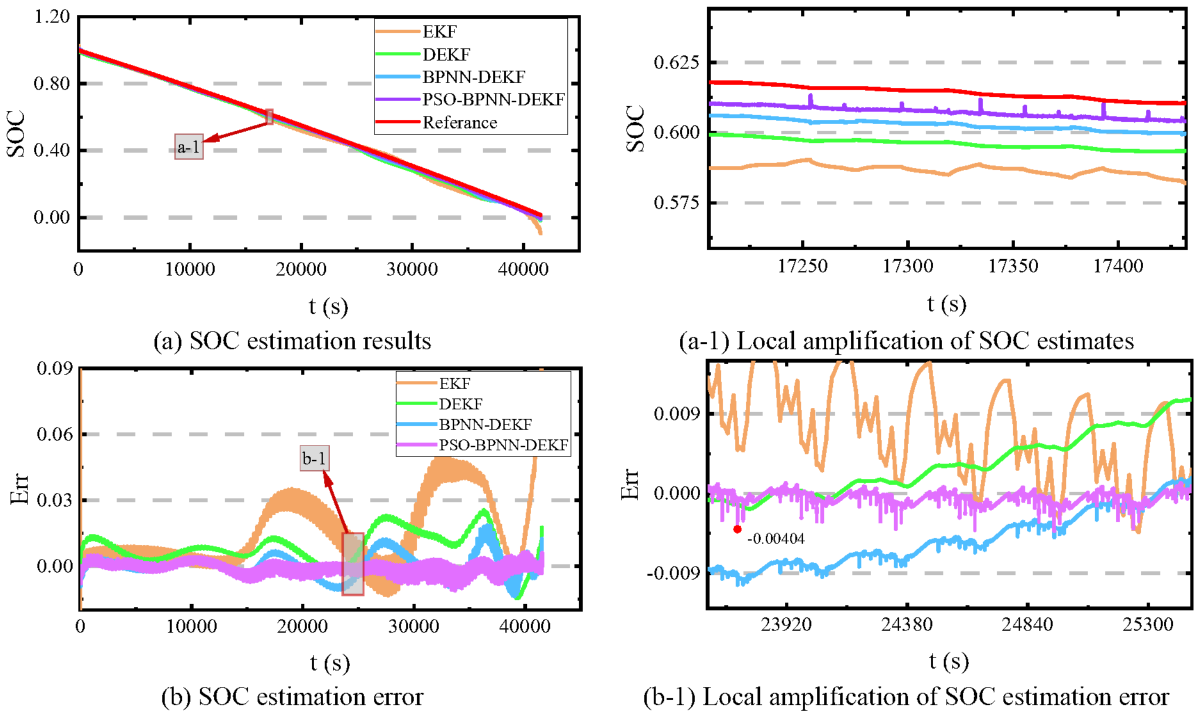

(a) SOC estimation results (a-1) Local amplification of SOC estimates

(b) SOC estimation error (b-1) Local amplification of SOC estimation error

Figure 10. SOC estimation results under BBDST working condition

From the SOC estimation curve and error curve obtained, it is obvious that both the EKF algorithm and DEKF algorithm can track the real SOC of batteries. Comparatively speaking, the SOC obtained by the DEKF algorithm is closer to the real value. DEKF joint estimation updates model parameters in real-time, which significantly inhibits the increase of error. To further compare the algorithm errors, after data processing, the algorithm errors in BBDST working conditions are shown in Table 6.

As can be seen from Table 6, MAE and RMSE for SOC estimation by EKF are 1.66% and 2.34%, respectively. DEKF adopted cyclic dual channels for state estimation and parameter update at the same time, which suppressed the estimation error to a certain extent. At this time, MAE and RMSE estimated by SOC were 0.95% and 1.13%, respectively, and 57.23% and 48.29% of MAE and RMSE estimated by EKF, respectively. After BPNN correction, DEKF estimated that MAE and RMSE of SOC decreased from 0.95% and 1.13% to 0.42% and 0.54%, respectively, and MAE and RMSE of BPNN-DEKF were only 44.21% and 47.78% of DEKF. It can be seen that BPNN is effective in correcting SOC estimation, further improving the accuracy of SOC estimation. The accuracy of SOC estimation is greatly improved after the error correction of SOC estimation by PSO-BPNN. At this point, MAE and RMSE for SOC estimation by PSO-BPNN-DEKF are 0.11% and 0.14%, respectively. MAE and RMSE of PSO-BPNN-DEKF are 26.19% and 25.92% of BPNN-DEKF, respectively.

Table 6. Comparison of SOC estimation errors of different algorithms under BBDST conditions

Method	MAE	RMSE	MAPE
EKF	0.0166	0.0234	0.1166
DEKF	0.0095	0.0113	0.1681
BPNN-DEKF	0.0042	0.0054	0.1081
PSO-BPNN-DEKF	0.0011	0.0014	0.0118

Figure. 11 and Figure. 12 respectively show the SOC estimation results after PSO-BPNN correction under DST and HPPC working conditions. It can be seen from the SOC estimation results under different working conditions that the SOC estimation results under HPPC and DST conditions are similar to those under BBDST conditions. All SOC estimated MAE after PSO-BPNN correction is limited to about 0.1%. It can be proved that the accuracy and superiority of the PSO-BPNN-DEKF algorithm for SOC estimation and correction under three dynamic tests. The MAE and RMSE estimated by SOC under DST and HPPC tests are shown in Table 7.

Table 7. Comparison of SOC estimation errors of different algorithms under DST conditions

	DST			**HPPC**		
Method	MAE	RMSE	MAPE	MAE	RMSE	MAPE
EKF	0.0173	0.0214	0.1065	0.01110	0.0142	0.0315
DEKF	0.0093	0.0114	0.1487	0.00530	0.0065	0.0121
BPNN-DEKF	0.0022	0.0044	0.0180	0.00190	0.0031	0.0052
PSO-BPNN-DEKF	0.0012	0.0036	0.0065	0.00045	0.0017	0.0010

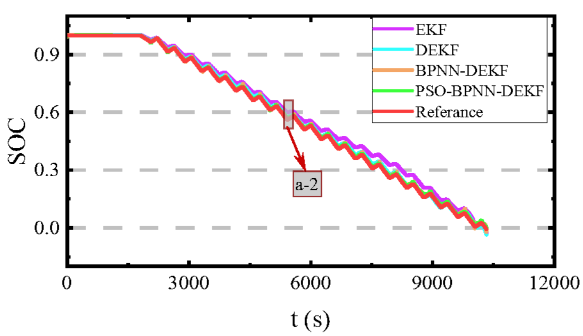

(a) SOC estimation results

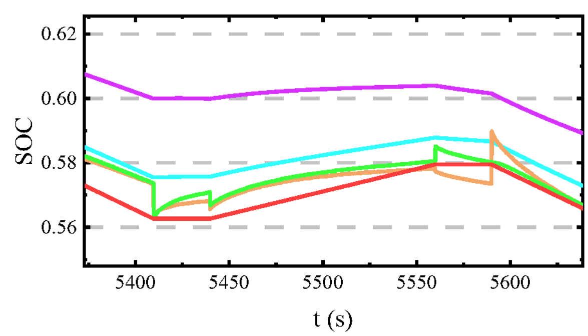

(a-2) Local amplification of SOC estimates

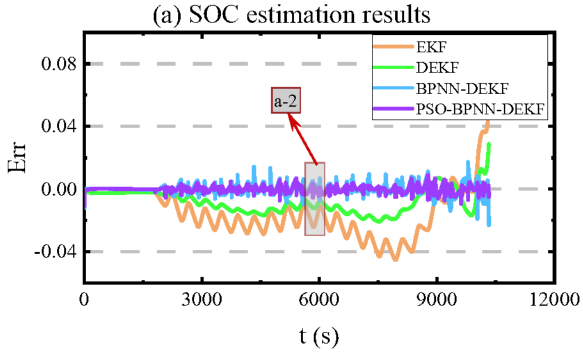

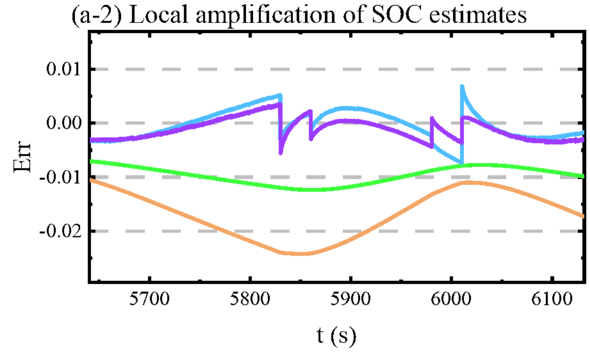

(b) SOC estimation error (b-2) Local amplification of SOC estimation error

Figure 11. SOC estimation results under DST working condition

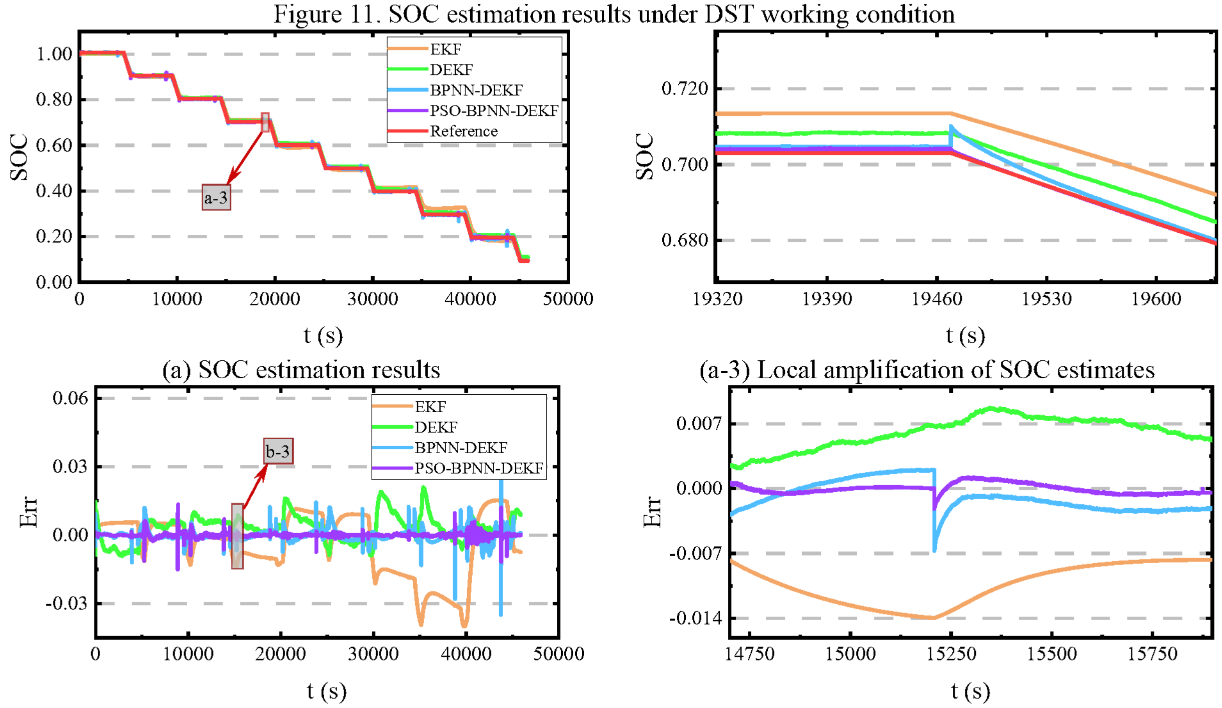

(a) SOC estimation results (a-3) Local amplification of SOC estimates

(b) SOC estimation error (b-3) Local amplification of SOC estimation error

Figure 12. SOC estimation results under HPPC working condition

From EKF to DEKF, SOC estimated MAE and RMSE were both reduced by about 1/2. From DEKF to PSO-BPNN-DEKF, MAE, and RMSE decreased by 87.10% and 68.42% respectively under DST condition. MAE and RMSE decreased by 91.39% and 73.85% respectively under HPPC condition.

The experimental results verify the effectiveness and accuracy of DEKF online parameter identification and PSO-BPNN for error correction and the superiority of PSO-BPNN for SOC correction. The above results further verify the accuracy and effectiveness of the proposed PSO-BPNN-DEKF algorithm for SOC estimation and correction.

3.5.2 SOC estimation results under different temperature conditions

To verify the accuracy of SOC estimation by PSO-BPNN-DEKF considering the temperature factor. In this study, BBDST dynamic operating conditions were tested at 15℃, 25℃, and 35℃. PSO-BPNN-DEKF algorithm was used to estimate and correct SOC under different temperature conditions. SOC estimation results under different temperature conditions are shown in Figure 13. SOC estimation errors under different temperature conditions are shown in Table 8.

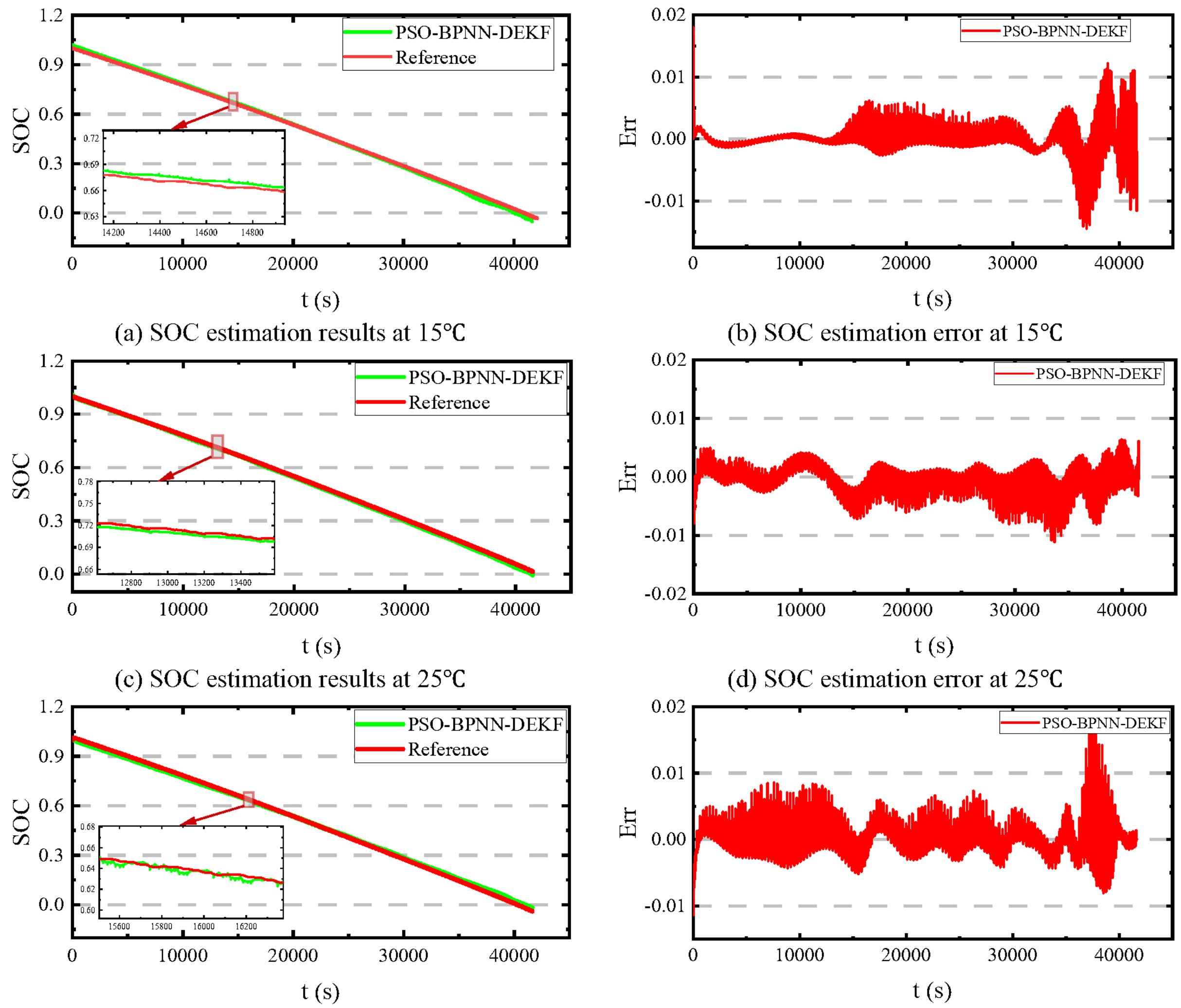

(a) SOC estimation results at 15℃
(b) SOC estimation error at 15℃
(c) SOC estimation results at 25℃
(d) SOC estimation error at 25℃
(e) SOC estimates at 35 ° C
(f) SOC estimation error at 35℃

Figure 13. SOC estimation results under BBDST dynamic working conditions under different temperature conditions

As can be seen from Figure 13, SOC estimation error basically stays within 0.01 at 15℃, 25℃, and 35℃. The above test results prove that PSO-BPNN-DEK can achieve relatively accurate SOC estimation under the three selected constant temperature conditions.

Table 8 SOC estimation errors under BBDST dynamic working conditions at different temperatures

Temperature	MAE	RMSE	MAPE
15℃	0.0011	0.0023	0.0572
25℃	0.0011	0.0014	0.0118
35℃	0.0012	0.0016	0.0105

Through the analysis of error data, it can be found that the MAE of SOC estimated by PSO-BPNN-DEKF is about 0.1% under different temperature conditions. RMSE is also limited to 0.25%. Experimental results show that PSO-BPNN-DEKF can also accurately estimate and correct SOC under different temperature conditions.

4. Conclusion

Based on the modeling of a second-order RC equivalent circuit, a simple AFFRLS is proposed to identify battery parameters with high precision. The PSO-BPNN-DEKF algorithm is proposed for SOC estimation and correction. The DEKF algorithm is used to estimate SOC and update model parameters online. The influence of parameter time variation on the accuracy of SOC estimation is reduced. PSO-BPNN is used to predict SOC estimation error in real time and compensate for the SOC estimation error of the DEKF algorithm. The accuracy of parameter identification is verified under BBDST conditions, and the accuracy of model identification based on the AFFRLS algorithm is improved by 1/2. The effectiveness and adaptability of the proposed algorithm are verified under BBDST, DST working conditions, and HPPC tests. The estimated error of SOC after correction is less than 0.015 under the three working conditions. Under BBDST and DST conditions, the estimated MAE of SOC after correction is only about 1/8 of that under DEKF. Under HPPC conditions, the estimated MAE of SOC after correction is only about 1/10 of that under DEKF. Under BBDST conditions with different temperatures, the estimated error of SOC after correction is about 0.1%. The applicability and superiority of the PSO-BPNN-DEKF algorithm in SOC estimation are verified. The experimental results show that the proposed PSO-BPNN-DEKF algorithm greatly improves the SOC estimation accuracy and is suitable for a variety of complex operating conditions and temperature conditions. This study provides a theoretical basis for real-time SOC estimation of battery management systems, which is conducive to promoting the development of new energy vehicle battery management systems.

Acknowledgments

The work is supported by the National Natural Science Foundation of China (No. 62173281, 61801407), Sichuan Sci ence and Technology Program (No. 23ZDYF0734, 23NSFSC4444).

Reference

1. Xing, L., L. Ling, and X. Wu, *Lithium-ion battery state-of-charge estimation based on a dual extended Kalman filter and BPNN correction.* Connection Science, 2022. 34(1): p. 2332-2363.
2. Li, Y., et al., *Recursive modeling and online identification of lithium-ion batteries for electric vehicle applications.* Science China Technological Sciences, 2014. 57(2): p. 403-413.
3. Wang, H., Y. Zheng, and Y. Yu, *Joint Estimation of SOC of Lithium Battery Based on Dual Kalman Filter.* Processes, 2021. 9(8), 1412: p. 1-10.
4. Qays, M.O., et al., *Recent Progress and Future Trends on the State of Charge Estimation Methods to Improve Battery-storage Efficiency: A Review.* Csee Journal of Power and Energy Systems, 2022. 8(1): p. 105-114.
5. Xiong, X., et al., *A novel practical state of charge estimation method: an adaptive improved ampere-hour method based on composite correction factor.* International Journal of Energy Research, 2020. 44(14): p. 11385-11404.
6. Liu, Z., et al., *Accurate and Efficient Estimation of Lithium-Ion Battery State of Charge with Alternate Adaptive Extended Kalman Filter and Ampere-Hour Counting Methods.* Energies, 2019. 12(4), 757: p. 1-15.
7. Xie, J., J. Ma, and K. Bai, *Enhanced Coulomb Counting Method for State-of-Charge Estimation of Lithium-ion Batteries based on Peukert's Law and Coulombic Efficiency.* Journal of Power Electronics, 2018. 18(3): p. 910-922.
8. Gismero, A., E. Schaltz, and D.-I. Stroe, *Recursive State of Charge and State of Health Estimation Method for Lithium-Ion Batteries Based on Coulomb Counting and Open Circuit Voltage.* Energies, 2020. 13(7), 1811: p. 1-11.
9. Knap, V. and D.-I. Stroe, *Effects of open-circuit voltage tests and models on state-of-charge estimation for batteries in highly variable temperature environments: Study case nano-satellites.* Journal of Power Sources, 2021. 498, 229913: p. 1-10.
10. Duan, J., et al., *State of Charge Estimation of Lithium Battery Based on Improved Correntropy Extended Kalman Filter.* Energies, 2020. 13(16), 4197: p. 1-18.
11. Kwak, M., et al., *A Variable-length scale Parameter Dependent State of Charge Estimation of Lithium Ion Batteries by Kalman Filters.* International Journal of Electrochemical Science, 2022. 17(2), 220218: p. 1-23.
12. Sun, Q., et al., *Adaptive Unscented Kalman Filter with Correntropy Loss for Robust State of Charge Estimation of Lithium-Ion Battery.* Energies, 2018. 11(11), 3123: p. 1-20.
13. Li, R., W. Li, and H. Zhang, *State of Health and Charge Estimation Based on Adaptive Boosting integrated with particle swarm optimization/support vector machine (AdaBoost-PSO-SVM) Model for Lithium-ion Batteries.*

International Journal of Electrochemical Science, 2022. 17(2), 03: p. 1-17.

14. Liu, B., et al., *State of charge estimation for lithium-ion batteries based on improved barnacle mating optimizer and support vector machine.* Journal of Energy Storage, 2022. 55, 105830: p. 1-12.

15. Song, Q., et al., *A Novel Joint Support Vector Machine - Cubature Kalman Filtering Method for Adaptive State of Charge Prediction of Lithium-Ion Batteries.* International Journal of Electrochemical Science, 2021. 16(8), 210823: p. 1-15.

16. Guo, N., et al., *Research on SOC fuzzy weighted algorithm based on GA-BP neural network and ampere integral method.* Journal of Engineering-Joe, 2019(15): p. 576-580.

17. Wang, Q., P. Wu, and J. Lian, *SOC estimation algorithm of power lithium battery based on AFSA-BP neural network.* Journal of Engineering-Joe, 2020. 2020(13): p. 535-539.

18. Zhang, X., et al., *Joint SOH-SOC Estimation Model for Lithium-Ion Batteries Based on GWO-BP Neural Network.* Energies, 2023. 16(1), 132: p. 1-17.

19. Zhang, J., Y. Wei, and H. Qi, *State of charge estimation of LiFePO4 batteries based on online parameter identification.* Applied Mathematical Modelling, 2016. 40(11-12): p. 6040-6050.

20. Liu, D., et al., *A novel fuzzy-extended Kalman filter-ampere-hour (F-EKF-Ah) algorithm based on improved second-order PNGV model to estimate state of charge of lithium-ion batteries.* International Journal of Circuit Theory and Applications, 2022. 50(11): p. 3811-3826.

21. Tian, J., et al., *Battery state-of-charge estimation amid dynamic usage with physics-informed deep learning.* Energy Storage Materials, 2022. 50: p. 718-729.

22. Zhang, D., et al., *Deep Learning in the State of Charge Estimation for Li-Ion Batteries of Electric Vehicles: A Review.* Machines, 2022. 10(10), 912: p. 1-21.

23. Bian, C., H. He, and S. Yang, *Stacked bidirectional long short-term memory networks for state-of-charge estimation of lithium-ion batteries.* Energy, 2020. 191, 116538: p. 1-10.

24. Fan, X., et al., *SOC estimation of Li-ion battery using convolutional neural network with U-Net architecture.* Energy, 2022. 256, 124612: p. 1-9.

25. Bian, C., S. Yang, and Q. Miao, *Cross-Domain State-of-Charge Estimation of Li-Ion Batteries Based on Deep Transfer Neural Network With Multiscale Distribution Adaptation.* Ieee Transactions on Transportation Electrification, 2021. 7(3): p. 1260-1270.

26. Zheng, F., et al., *Influence of different open circuit voltage tests on state of charge online estimation for lithium-ion batteries.* Applied Energy, 2016. 183: p. 513-525.

27. Lulu, L., et al., *Research on fractional modeling and SOC eatimation strategy of Lithium battery.* Energy Storage Science and Technology, 2022. 2(12): p. 544-551.

28. Xiaoyang, Z., C. Kangyi, and W. Xinbo, *SOC estimation algorithm of lithium battery based on simplified fractional order AEPF.* Chinese Journal of Power Sources, 2022. 46(10): p. 1156-1160.

29. Zheng, L., et al., *Differential voltage analysis based state of charge estimation methods for lithium-ion batteries using extended Kalman filter and particle filter.* Energy, 2018. 158: p. 1028-1037.

30. Nian, P., Z. Shuzhi, and Z. Xiongwen, *Co-estimation for capacity and state of charge for lithium-ion batteries using improved adaptive extended Kalman filter.* Journal of Energy Storage, 2021. 40, 102559: p. 1-15.

31. Yi, H., et al., *An Innovative State-of-charge Estimation Method of Lithium-ion Battery Based on 5th-order Cubature Kalman Filter.* Automotive Innovation, 2021. 4(4): p. 448-458.

32. Biying, R., et al., *Lithium-ion battery parameter identification based on VFFRLS with wavelet transform.* Journal of Xi'an University of Technology, 2022. 38(01): p. 133-141.

33. Ge, C., Y. Zheng, and Y. Yu, *State of charge estimation of lithium-ion battery based on improved forgetting factor recursive least squares-extended Kalman filter joint algorithm.* Journal of Energy Storage, 2022. 55, 105474: p. 1-7.

34. Ji, S., et al., *A Multi-Scale Time Method for the State of Charge and Parameter Estimation of Lithium-Ion Batteries Using MIUKF-EKF.* Frontiers in Energy Research, 2022. 10, 933240: p. 1-9.

35. Su, J., et al., *An equivalent circuit model analysis for the lithium-ion battery pack in pure electric vehicles.* Measurement & Control, 2019. 52(3-4): p. 193-201.

36. Vishnu, C. and A. Saleem, *Adaptive Integral Correction-Based State of Charge Estimation Strategy for Lithium-Ion Cells.* Ieee Access, 2022. 10: p. 69499-69510.

37. Jinlei, S., et al., *State of Charge Estimation for Lithium-ion Battery Based on FFRLS-EKF Joint Algorithm.* Automotive Engineering, 2022. 44(04): p. 505-513.

38. Xing, L., et al., *State-of-charge estimation for Lithium-Ion batteries using Kalman filters based on fractional-order models.* Connection Science, 2022. 34(1): p. 162-184.

39. Priya, R.P., S. R, and R. Sakile, *State of charge estimation of lithium‐ion battery based on extended Kalman filter and unscented Kalman filter techniques.* Energy Storage, 2022. 5(3): p. 1-16.

40. Yuan, H., et al., *State of Charge Estimation of Lithium Battery Based on Integrated Kalman Filter Framework and Machine Learning Algorithm.* Energies, 2023. 16(5), 2155: p. 1-16.